



Trans. Nonferrous Met. Soc. China 21(2011) 2764-2771

Transactions of Nonferrous Metals Society of China

www.tnmsc.cn

# Adsorption of ytterbium (III) from aqueous solution by SQD-85 resin

XIONG Chun-hua, WANG Guo-tao, YAO Cai-ping

Department of Applied Chemistry, Zhejiang Gongshang University, Hangzhou 310012, China

Received 13 December 2010; accepted 16 May 2011

**Abstract:** Adsorption and desorption behavior of Yb (III) by SQD-85 resin was investigated by various chemical methods and IR spectrometry. The adsorption capacity of SQD-85 resin for Yb (III) was studied as a function of solution pH, initial concentration of Yb(III), temperature and contact time. The optimal pH for the adsorption was 5.50 in the HAc-NaAc system, and the maximum adsorption capacity was estimated to be 347.6 mg/g at 308 K. The isotherms adsorption data fit well with Langmuir model. The adsorption kinetics data are in agreement with pseudo-second-order model. Thermodynamic parameters indicate that Yb (III) adsorption by SQD-85 resin is endothermic and spontaneous in nature. Thomas model is reasonably accurate in predicting experimental column results. The dynamic desorption rate of Yb(III) can increase to 97.3% when the elution agent is 1.0 mol/L HCl. These results suggest that Yb(III) in aqueous solution can be removed and recovered by SQD-85 resin efficiently.

Key words: SQD-85 resin; adsorption; Yb(III); kinetics; thermodynamics; mechanism

#### 1 Introduction

Rare earth elements (REEs) are being increasingly used as important components in lasers, phosphors, magnetic bubble memory films, refractive index lenses, fiber optics, superconductors, high-intensity lightning, coloured glasses, refining industry and nuclear technology [1–5]. Ytterbium is an important member of rare-earth family and widely used in various fields. However, REEs, including ytterbium, have a low to moderate acute toxicity rating. In some studies, it has been found that intraperitoneal administration of ytterbium with concentrations of above 0.01% in the diet for 90 d, produced liver and spleen damage [6]. Ytterbium compounds are also known to cause skin and eye irritation and may be teratogenic [7].

Several techniques, such as chemical precipitation, ion exchange, membrane separation, reverse osmosis and extraction chromatography have been reported for the adsorption and separation of REEs from aqueous solution [8–13]. Compared with the other methods, ion exchange has received a considerable attention in recent years because it is simple, relatively low-cost and effective [14–16]. SQD–85 macroporous weak acid resin

is a novel polymeric material. It not only has the proton that can exchange with cation, but also has oxygen atom that can coordinate directly with metal ions. It is as well widely available as it is commercially produced. Furthermore, its regeneration properties supply economical benefits. Due to mentioned properties, SQD-85 resin has been preferred in this study.

Batch and column experiments were performed to test the feasibility of removal and recovery of Yb(III) from aqueous solution by using the SQD-85 resin. Some factors affecting adsorption, such as pH of solution, initial concentration of Yb(III), contact time and temperature were examined. Kinetics and isotherms adsorption experiments were carried out Thermodynamic parameters of adsorption for Yb(III) were calculated. The resin was also characterized with FT-IR spectroscopy. It is thought that results of this study can be useful for treatment processes of sector containing REEs in their wastewater.

## 2 Experimental

# 2.1 Apparatus

The concentration of Yb(III) in solution was determined with Shimadzu UV-2550 UV-visiable spectro-

Foundation item: Project (2011007) supported by Key Laboratory of Advanced Textile Materials and Manufacturing Technology of Ministry of Education,
Zhejiang Sci-tech University, China; Project (2010C32085) supported by Science and Technology Department of Zhejiang Province,
China

photometer. The resin dosage was measured by electronic balance of Sartorius BS 224S. Mettler toledo delta 320 pH meter was used for measuring pH of solution. The sample was shaken in the DSHZ-300A and the THZ-C-1 electrically thermostated reciprocating shaking machine. The IR spectrum was detected on Nicolet 380 FT-IR spectrometer. The water used in the present work was purified using Molresearch analysistype ultra-pure water machine.

#### 2.2 Materials

SQD-85 resin was supplied by Jiangsu Suqing Water Treatment Engineering Group Co., Ltd. and the properties are shown in Table 1. Standard solution of metal ions was prepared from ytterbia (AR). HAc-NaAc buffer solution with pH 4.00-6.50 and C<sub>6</sub>H<sub>15</sub>O<sub>3</sub>N-HNO<sub>3</sub> buffer solution with pH 7.20 were prepared from the NaAc, HAc, C<sub>6</sub>H<sub>15</sub>O<sub>3</sub>N and HNO<sub>3</sub> solutions. The chromophoric reagent of 0.1% arsenazo-I solution was obtained by dissolving 0.1000 g arsenazo-I powder into 100 mL purified water. All other chemicals were of analytical grade and purified water was used throughout.

#### 2.3 Adsorption experiments

Experiments were run in a certain range of pH, initial concentration of Yb(III), temperature, contact time as well as adsorption isotherms. The operations for the adsorption and desorption of Yb(III) were carried out in batch vessels and glass columns.

Batch experiments were performed under kinetics and equilibrium conditions. A desired amount of treated SQD-85 resin was weighed and added into a conical flask, in which a desired volume of buffer solution with pH 5.50 was added. After 24 h, a required amount of standard solution of Yb(III) was put in. The flasks were shaken in a shaker at constant temperature and rotation speed. The upper layer of clear solution was taken for analysis until adsorption equilibrium reached. The procedure of kinetics test was identical to that of the equilibrium test. The aqueous samples were taken at preset time intervals and the concentrations of Yb(III) were similarly measured.

In the column experiments, continuous packed bed studies were performed in a fixed bed mini glass column (d3 mm×300 mm) with SQD-85 resin and filled with the Yb(III) solution. At the bottom of the column, a stainless sieve was attached followed by a layer of cotton wool. The particles were dropped in from the top of the column. Time taken by the particles to travel a distance of resin

column in vertical direction was noted. The Yb(III) solutions at the outlet of the column were collected at regular time intervals and the concentrations of Yb(III) were measured.

#### 2.4 Analytical method

A solution containing a required amount of Yb(III) was added into a 25 mL colorimetric tube, and then 1.0 mL of 0.1% arsenazo-I solution and 10 mL pH 7.20  $C_6H_{15}O_3N$ -HNO $_3$  buffer solution were added, after the addition of purified water to the mark of the colorimetric tube, the absorbency was determined in an 1 cm colorimetric vessel at wavelength of 573 nm and compared with blank test. The adsorption capacity (Q, mg/g) and distribution coefficient (D, mL/g) were calculated with the following formulas:

$$Q = \frac{C_0 - C_e}{m} V \tag{1}$$

$$D = \frac{C_0 - C_e}{m \cdot C} V \tag{2}$$

where  $C_0$  is initial concentration in solution (mg/mL);  $C_e$  is equilibrium concentration in solution (mg/mL); V is solution volume of solution (mL); m is resin dry mass (g).

# 3 Results and discussion

## 3.1 Effect of pH

Many studies showed that pH value seems to be the most important parameter for controlling the adsorption process. The uptake of metal ions as a function of hydrogen ion concentration was in the range of pH 4.00–6.50 for an initial concentration of 0.233 mg/mL at 298 K and 100 r/min. The effect of pH on the adsorption behavior is illustrated in Fig. 1.

The adsorption capacity of Yb(III) was the highest when pH was 5.50 in the HAc-NaAc medium and decreased by either raising or lowering pH under the experimental condition. The pH value affected the surface charge of the adsorbent and the degree of ionization of the adsorbate in aqueous solution. The Yb(III) uptake can increase as the pH went up, and it can be explained based on a decrease in competition between protons (H<sup>+</sup> ion) and metal cations (Yb(III) ion) for the same adsorption sites and by the decrease in the positive surface charge on the resin resulting in a lower electrostatic repulsion between the surface of resin and Yb(III). Contrarily, the Yb(III) was prone to chemical

Table 1 General description and properties of SQD-85 resin

Resin	Functional group	Structure	Moisture/%	Wet superficial density/(g·mL <sup>-1</sup> )	True wet density/ $(g \cdot mL^{-1})$
Macroporous weak acid resin	—соон	Macroporous	45-50	0.70-0.80	1.10-1.20

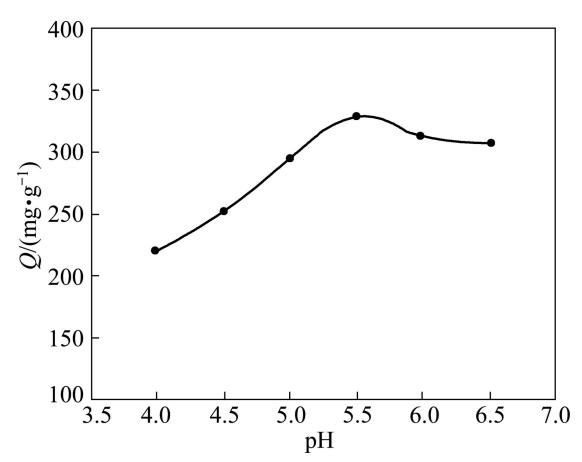
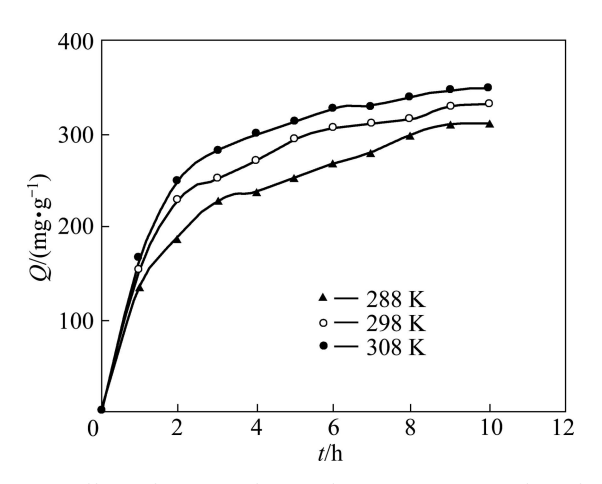


Fig. 1 Effect of pH on adsorption capacity of Yb(III) onto SQD-85 resin (resin 15.0 mg, T = 298 K,  $C_0 = 0.233 \text{ mg/ mL}$ )

precipitation at higher pH values [17]. Therefore, the subsequent adsorption experiments were carried out at pH 5.50 in HAc-NaAc system.

#### 3.2 Effect of contact time

The influence of contact time on the adsorption of Yb(III) onto SQD-85 resin was investigated at the temperatures of 288, 298 and 308 K. Each series of experiments were performed on 60.0 mL mixture solution of buffer solution and Yb(III) solution and 30.0 mg of SQD-85 resin shaken in conical flask. At predetermined intervals, aliquots of 0.3 mL solution was taken out for analysis and the concentrations of Yb(III) were determined. After the remains kept constant and volume was corrected, a series of data were obtained as shown in Fig. 2.



**Fig. 2** Effect of contact time and temperature on adsorption capacity of Yb(III) onto SQD-85 resin (resin 30.0 mg,  $C_0$ =0.233 mg/mL)

It was found that the adsorption capacity increased with contact time. The loading half time  $t_{1/2}$  was less than 2 h and the maximum adsorption was observed after 10 h, beyond which there was almost no change in the

adsorption. Therefore, this interaction time could be very well taken as the equilibrium time. Meanwhile, the equilibrium adsorption capacity of Yb(III) onto SQD-85 resin was found to increase from 310.9 to 347.6 mg/g, when temperature rose from 288 K to 308 K, indicating that the adsorption of Yb(III) onto the adsorbent was favored at higher temperature. This effect suggests that the adsorption mechanism associated with Yb(III) onto SQD-85 resin involves a temperature dependent process.

#### 3.3 Adsorption kinetics

Several kinetics models are needed to examine the mechanism of adsorption process from a liquid phase on the SQD-85 resin and to interpret the experimental data. The Lagergren first-order model [18] can be expressed as

$$\lg(Q_{e} - Q_{t}) = \lg Q_{1} - \frac{k_{1}}{2303}t \tag{3}$$

The pseudo-second-order model [19] can be expressed as

$$\frac{t}{Q_t} = \frac{1}{k_2 Q_2^2} + \frac{t}{Q_2} \tag{4}$$

where  $Q_e$  and  $Q_t$  are the amounts of Yb(III) adsorbed on the adsorbent at equilibrium and at various time (mg/g), respectively;  $Q_1$  and  $Q_2$  are the calculated adsorption capacity of the Lagergren first-order model and the pseudo-second-order model (mg/g), respectively;  $k_1$  and  $k_2$  are the rate constants of the Lagergren first-order model (min<sup>-1</sup>) and the pseudo-second-order model (g/(mg·min)), respectively. The fitting validity of these models is traditionally checked by the linear plots of  $\lg(Q_e - Q_t)$  versus t, and  $t/Q_t$  versus t, respectively.

The pseudo-second-order model assumes that the rate limiting step may be chemisorption involving valency forces through sharing or exchange of electron between the sorbent and the sorbate. As shown in Table 2, the correlation coefficient  $R_2^2$  for the pseudo-second-order model is higher than the correlation coefficient  $R_1^2$  for the Lagergren first-order model. This means that the pseudo-second-order model can describe the Yb(III)/SQD-85 resin adsorption system studied in our work, and the rate controlling step of the adsorption process is governed by chemisorption [20].

## 3.4 Adsorption isotherms

Adsorption isotherms describe how adsorbates interact with adsorbents. Therefore, the correlation of equilibrium data by either theoretical or empirical equations is also essential to the practical design and operation of adsorption systems. Adsorption isotherms models were conducted as follows: four parts of 15.0 mg of SQD-85 resin and four parts of Yb(III) solutions with the initial concentrations of 0.133, 0.167,

TIV.	o // =1>	Lagergren first-order model		Pseudo-second-order model	
T/K	$Q_{\rm e}/({ m mg\cdot g}^{-1})$	$k_1/10^{-3} \mathrm{min}^{-1}$	$R_1^2$ $k_2/(10^-$	$k_2/(10^{-5} \text{g·mg}^{-1} \cdot \text{min}^{-1})$	$R_2^2$
288	310.9	7.955	0.8048	2.414	0.9986
298	322.7	7.038	0.9290	3.059	0.9988
308	347.6	9.069	0.8673	3.400	0.9995

Table 2 Lagergren first-order and pseudo-second-order kinetics parameters

0.200 and 0.233 mg/mL were shaken in flasks until equilibrium at pH 5.5, 288–308 K and 100 r/min.

Adsorption isotherms of Yb(III) at different temperatures are depicted in Fig. 3. With increasing concentration of solution, adsorption capacity increased. Several adsorption isotherms models were available and the two important isotherms models (Langmuir, Freundlich) were selected in this study. Langmuir isotherms model is expressed as

$$\frac{C_{\rm e}}{Q_{\rm e}} = \frac{1}{Q_{\rm m}K_{\rm L}} + \frac{C_{\rm e}}{Q_{\rm m}} \tag{5}$$

where  $K_{\rm L}$  is the Langmuir constant which can be considered a measured adsorption energy and  $Q_{\rm m}$  is the maximum adsorption capacity corresponding to complete monolayer coverage (mg/g). A plot of  $C_{\rm e}/Q_{\rm e}$  versus  $C_{\rm e}$  over the entire concentration range produces a straight line, which is an indication of the applicability of the Langmuir isotherms for the system under consideration. Freundlich isotherms model is expressed as

$$\lg Q_{\rm e} = \frac{1}{n} \lg C_{\rm e} + \lg K_{\rm F} \tag{6}$$

where  $K_F$  is the Freundlich constant, and n is an empirical constant related to the magnitude of the adsorption driving force. The intercept and the slope of the linear plot of  $\lg C_e$  versus  $\lg Q_e$  at given experimental conditions provide the values of  $K_F$  and 1/n, respectively.

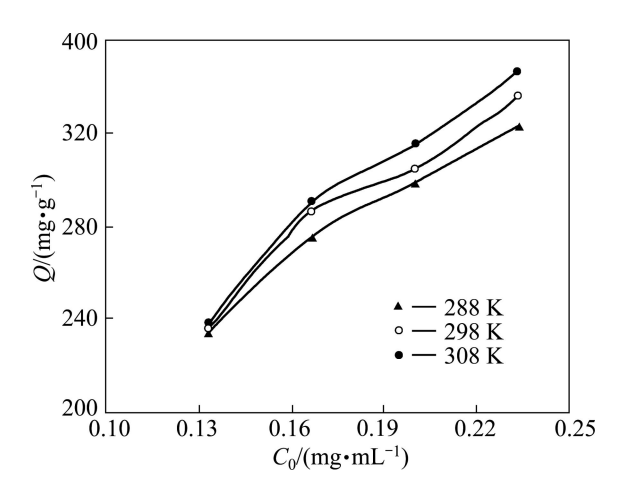


**Fig. 3** Effect of initial Yb(III) concentration on adsorption capacity at different temperatures (resin 15.0 mg)

The Langmuir isotherms model assumes that adsorption takes place at specific homogeneous sites within the adsorbents and has been successfully applied to many other real adsorption processes. The calculated values of Langmuir constants ( $Q_m$  and  $K_L$ ) are listed in Table 3. Langmuir constant  $(Q_m)$  was 391.5 mg/g which represented the maximum monolayer adsorption capacity of SQD-85 resin for Yb(III) sorption at 308 K. The increase of  $Q_m$  with the temperature rise signifies that the process needed thermal energy (endothermic) and there was a chemical interaction between adsorbent and adsorbate [21]. The correlation coefficient  $R_{\rm I}^2 > 0.99$ indicated the applicability of Langmuir isotherms model for the adsorption data. However, the Freundlich isotherms model describes equilibrium on heterogeneous surfaces and hence does not assume monolayer capacity. The values of Freundlich constants (n and  $K_F$ ) are also listed in Table 3. The values of n greater than 1 indicate favorable adsorption conditions. In most cases, the exponent  $1 \le n \le 10$  shows beneficial adsorption [22].

 Table 3
 Langmuir and Freundlich adsorption isotherms

 parameters

T/K	Langmuir			F	Freundlich		
	$Q_{\rm m}/({\rm mg}\cdot{\rm g}^{-1})$	$K_{\rm L}$	$R_{\rm L}^{2}$	$K_{\mathrm{F}}$	n	$R_{\rm F}^{2}$	
288	359.7	113.6	0.9912	554.4	4.90	0.9196	
298	373.0	120.2	0.9989	593.9	4.75	0.9962	
308	391.5	113.3	0.9933	681.1	4.21	0.9513	

#### 3.5 Adsorption thermodynamics

The effect of temperature on the adsorption of Yb(III) onto SQD-85 resin was also studied in the range of 288–308 K under optimum conditions. There are three important thermodynamic parameters, i.e., changes in enthalpy ( $\Delta H$ ), entropy ( $\Delta S$ ) and Gibb's free energy ( $\Delta G$ ), respectively. They were estimated using the following relationships [23]:

$$\lg D = -\frac{\Delta H}{2.303RT} + \frac{\Delta S}{2.303R} \tag{7}$$

$$\Delta G = \Delta H - T \Delta S \tag{8}$$

where D is distribution coefficient; R is the gas constant; and T is the absolute temperature. A linear plot was obtained by plotting  $\lg D$  versus 1/T as shown in Fig. 4.

The linear equation was y=-0.4939x+5.3672 and the correlation coefficient was 0.998. The values of  $\Delta H$ ,  $\Delta S$  and  $\Delta G$  were estimated using the relationships. The calculation results are listed in Table 4.

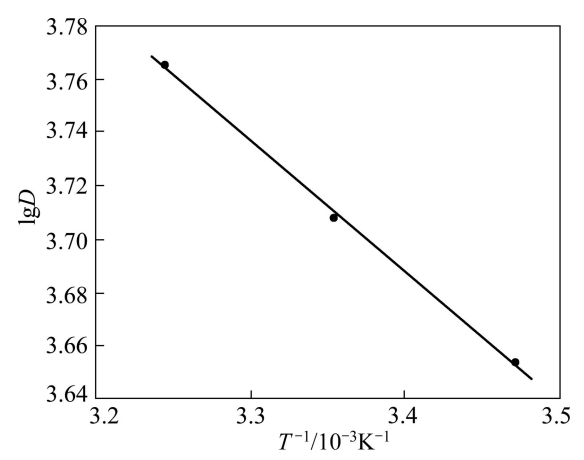


**Fig. 4** Effect of temperature on distribution ratio (resin 15.0 mg,  $C_0$ =0.233 mg/mL)

**Table 4** Thermodynamic parameters for Yb(III) onto SQD-85 resin

$\Delta H$ /	$\Delta S$ /	$\Delta G/(\mathrm{kJ \cdot mol}^{-1})$		1)
$(kJ \cdot mol^{-1})$	$(J \cdot K^{-1} \cdot mol^{-1})$	288 K	298 K	308 K
9.46	102.00	-29.36	-30.38	-31.40

The positive values of  $\Delta S$  (102.00 J/(K·mol)) referred to the increased randomness at the solid-solution interface. The positive values of  $\Delta H$  (9.46 kJ/mol) indicated that the adsorption process was an endothermic process, and significant changes may occur in the internal structure of the adsorbent through the adsorption. The negative value of  $\Delta G$  confirmed the feasibility of the process and spontaneous in nature of the adsorption process [24].

#### 3.6 Desorption

Efficient elution of adsorbed solute from resin is essential to ensure the reuse of resin for repeated adsorption-desorption cycles. To determine desorption properties of SQD-85 for Yb(III), the elute tests were designed. 15.0 mg SQD-85 resin was added into a mixed solution composed of pH 5.50 buffer solution and desired amount of Yb(III) solution. After equilibrium reached, the concentration of Yb(III) in the aqueous phase was determined, and the adsorption capacity of the SOD-85 resin for Yb(III) was obtained. Then, the SQD-85 resin separated from aqueous phase was washed three times with the buffer solution, and was shaken with 30.0 mL HCl eluant of different After concentrations. equilibrium reached, concentration of Yb(III) in aqueous phase determined and then the percentage of elution for Yb(III)

was obtained. Table 5 shows that the concentration of HCl increases the percentage of elution for Yb(III). The percentage can achieve 95.7%, so the Yb(III) adsorbed on SQD-85 resin can be recovered efficiently.

Table 5 Elution test of Yb(III) from loaded SQD-85 resin

	Concentration of	Elution amount/	Elution percentage/	
_	HCl/(mol·L <sup>-1</sup> )	mg	%	
	0.1	3.35	68.6	
	0.5	4.35	89.1	
	1.0	4.68	95.7	
	1.5	4.60	95.8	
	2.0	4.68	95.7	

Considering the environmental pollution and economic cost, the experimental results show that 1.0 mol/L HCl is the best.

#### 3.7 Column experiments

#### 3.7.1 Dynamic adsorption curve

The performance of packed bed is described through the concept of the breakthrough curve. The breakthrough curve shows the adsorption behaviour of Yb(III) from solution in a packed bed and is usually expressed in terms of adsorbed Yb(III) concentration  $(C_{\rm ad}=C_0-C_{\rm e})$  or normalized concentration defined as the ratio of effluent Yb (III) concentration to the inlet Yb(III) concentration  $(C_{\rm e}/C_0)$  as a function of time or volume of effluent for a given bed height [25]. The area under the breakthrough curve obtained by integrating the adsorbed concentration  $(C_{\rm ad})$  versus the throughput volume (V) plot can be used to find the total adsorbed Yb(III) quantity (the maximum column adsorption capacity). Total adsorbed Yb(III) quantity (Q) in the column for a given feed concentration and flow rate can be calculated from

$$Q = \int_0^v \frac{(C_0 - C_e)}{m} dV$$
 (9)

The obtained adsorption capacity Q was 348.2 mg/g according to Eq. (9). Successful design of a column adsorption process requires prediction of the concentration versus time profile or breakthrough curve for the effluent. The maximum sorption capacity is also in design. Traditionally, the Thomas model is used to fulfill the purpose. The model follows form:

$$\frac{C_{\rm e}}{C_0} = \frac{1}{1 + \exp\left[K_{\rm T}(Qm - C_0)/\theta\right]}$$
 (10)

where  $K_T$  is the Thomas rate constant and  $\theta$  is the volumetric flow rate. The linearized form of the Thomas model is as follows:

$$\ln\left(\frac{C_0}{C_e} - 1\right) = \frac{K_T Q m}{\theta} - \frac{K_T C_0}{\theta} V \tag{11}$$

The kinetics coefficient  $K_{\rm T}$  and the adsorption capacity Q of the column can be determined from a plot of  $\ln[(C_0/C_{\rm e})-1]$  versus t at a certain flow rate as shown in Fig. 5. The outlet time t is obtained from  $V/\theta$ . The Thomas equation coefficient for Yb(III) adsorption was  $K_{\rm T}=2.10\times10^{-2}$  mL/(min·mg) and theoretical Q was 359.3 mg/g. The theoretical predictions based on the model parameters were compared with the observed data as shown in Fig. 6. It was shown that the experimental data were well fitted by the model of Thomas model with the high  $R^2$  value (0.9717) and the calculated Q value was very close to the experimental data. The successful simulation of the experimental result demonstrates the validity of applying Thomas model for the design and simulation of column adsorption.

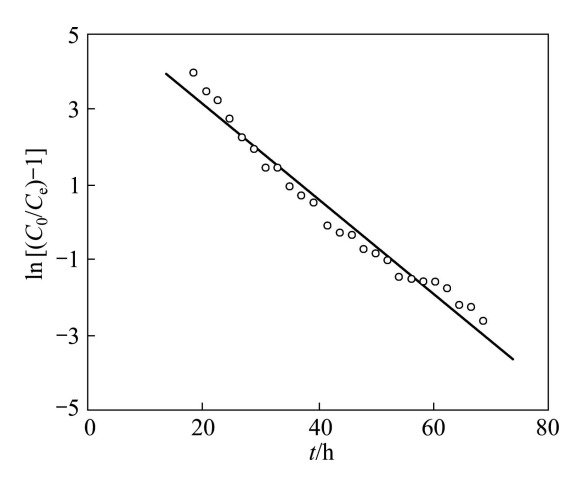


**Fig. 5** Linear plots of  $ln[(C_0/C_e)-1]$  versus t by application of Thomas model (resin 150.0 mg,  $C_0$ =0.100 mg/mL, flow rate 0.200 mL/min)

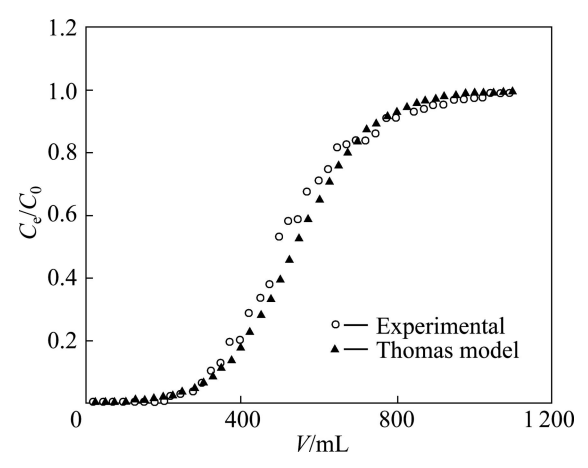


**Fig. 6** Experimental and predicted breakthrough curves using Thomas model for Yb(III) adsorption by SQD-85 resin (resin 150.0 mg,  $C_0$ =0.100 mg/mL, flow rate 0.200 mL/min)

#### 3.7.2 Dynamic desorption curve

With respect to the dynamic desorption of Yb(III) from SQD-85 resin, the 1.0 mol/L HCl eluant was employed. Desorption curve was plotted with the effluent concentration ( $C_e$ ) versus elution volume (V)

from the column at a certain flow rate. As shown in Fig.7, the total volume of eluent was 100 mL and the desorption process took 8.3 h, after which further desorption was negligible. The percentage of elution can reach 97.3 %. The volume of elution was significantly less than saturation volume, which was beneficial to the easy handling and it can obtain a relatively high concentration for economical recovery of Yb(III).

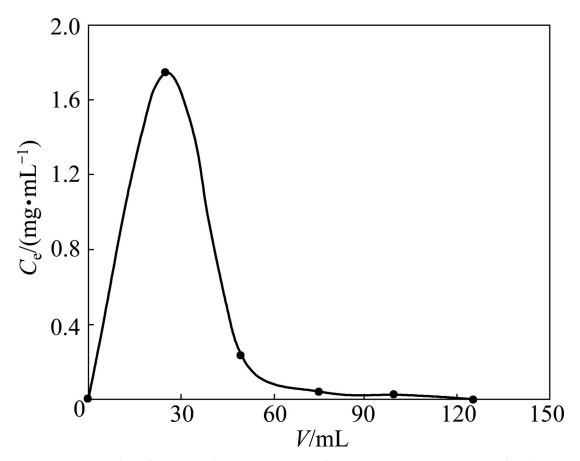


Fig. 7 Dynamic desorption curve (flow rate 0.200 mL/min)

#### 3.8 IR analysis

IR analysis is an important analytical tool for determination of adsorption mechanism. The information about structural changes caused by the SOD-85 resin loading with Yb (III) was given by FTIR spectra (Fig. 8). The spectrum of SQD-85 resin showed peaks at 3 439 cm<sup>-1</sup> assigned to stretching vibrations of hydroxyl groups; 2 931 cm<sup>-1</sup> assigned to the stretching vibrations of —CH<sub>2</sub>, —CH<sub>3</sub> groups; 1 712 cm<sup>-1</sup> assigned to stretching vibrations of C=O in -COOH groups; 1 403cm<sup>-1</sup> assigned to bending vibrations of O—H; 1 552 cm<sup>-1</sup> and 1 447 cm<sup>-1</sup> assigned to antisymmetric stretching vibration band and symmetric stretching vibration band of —COO— groups, respectively. After the adsorption, the characteristic peak of hydroxyl groups stretching vibrations shifted to lower frequency (from 3 448 cm<sup>-1</sup> to 3 427 cm<sup>-1</sup>), the peak at 1 710 cm<sup>-1</sup> decreased in intensity, and 1 403 cm<sup>-1</sup> was blue-shifted at 1 409 cm<sup>-1</sup>. These findings may suggest that the hydrogen and oxygen atoms in the —OH and C—O groups were involved in Yb(III) adsorption [26]. The adsorption mechanism might be partly a result of the ion exchange or complexation between the Yb(III) ions and carboxyl groups of SQD-85 resin. Thus, the Yb(III)/SQD-85 resin reaction may be represented in two ways as shown in Fig. 9 [27]. First, since the oxygen of the carboxyl has a pair of electrons that can add themselves to a proton or a metal ion to form a complex through a coordinated covalent bond, it takes us to propose that the complexes between metal ions (Yb(III)) and SOD-85 resin are formed according to the mechanism illustrated in

Fig. 9(a). Second, under acidic environment, the metal adsorption capacity diminishes as the solution pH decreases. This may be a result of the decrease of the retention efficiency of the absorbent due to the occupation of the active sites of the weak ion-exchanger by protons. The proposed mechanism is illustrated in Fig. 9(b). According to the FT-IR spectra, we can infer that these two adsorption ways co-exist in the same process under our experimental conditions.

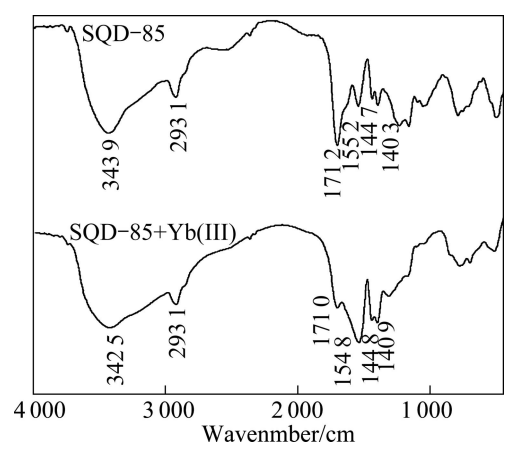
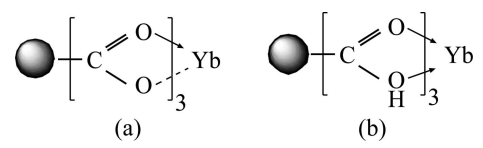


Fig. 8 FTIR spectra of SQD-85 resin before and after being loaded Yb (III)



**Fig. 9** Schematic diagram of proposed Yb(III) adsorption mechanism with SQD-85 resin: (a) Complexation and ion exchange; (b) Complexation

### 4 Conclusions

- 1) The adsorption of Yb(III) onto SQD-85 resin is highly dependent on pH of the medium as well as contact time and system temperature. The maximum adsorption capacity is estimated to be 347.6 mg/g in pH 5.50 HAc-NaAc system at 308 K. And it is found that 1.0 mol/L HCl solution provides effectiveness of the desorption of Yb(III) from SQD-85 resin.
- 2) The kinetics of adsorption of Yb(III) onto SQD-85 resin were tested with models based on the Lagergren first-order and pseudo-second-order. Close conformity can be obtained with pseudo-second-order mechanism.
- 3) The isotherms adsorption data are fitted better to the Langmuir model than Freundlich model. This suggests that the adsorption of Yb(III) onto SQD-85 resin is monolayer-type.
- 4) Thermodynamic parameters such as changes in the enthalpy ( $\Delta H$ ), entropy ( $\Delta S$ ) and Gibb's free energy ( $\Delta G$ ) indicate that Yb(III) adsorption onto SQD-85 resin

- is endothermic and spontaneous in nature.
- 5) Thomas model is reasonably accurate in predicting experimental column results for this work. Column experiments show that it is possible to removal and recovery Yb(III) from aqueous medium dynamically.
- 6) The FT-IR spectra of SQD-85 resin before and after the adsorption of Yb(III) show that hydrogen and oxygen atoms in the —OH and C—O groups are involved in Yb(III) adsorption.

#### References

- LEZHNINA M M, KYNAST U H. Optical properties of matrix confined species [J]. Optical Materials, 2010, 33(1): 4–13.
- [2] GARSKAITE E, LINDGREN M, EINARSRUD M A, GRANDE T. Luminescent properties of rare earth (Er, Yb) doped yttrium aluminium garnet thin films and bulk samples synthesised by an aqueous sol-gel technique [J]. Journal of the European Ceramic Society, 2010, 30(7): 1707–1715.
- [3] HANTZSCHE K, BOHLEN J, WENDT J, KAINER K U, YI S B, LETZIG D. Effect of rare earth additions on microstructure and texture development of magnesium alloy sheets [J]. Scripta Materialia, 2010, 63(7): 725–730.
- [4] JEAN CLANDE G B, ANNE-SOPHIE C, HWAN K K, EMMANUEL D, SVETLANA V E. Lanthanide luminescence efficiency in eight- and nine-coordinate complexes: Role of the radiative lifetime [J]. Coordination Chemistry Reviews, 2010, 254(21–22): 2623–2633.
- [5] HUANG Xiao-hua, ZHOU Qing. Application of rare earth in fertilizer [J]. Nature Magazine, 2001, 23(3): 160–163. (in Chinese)
- [6] SINGH A K, SINGH P. Nano-level monitoring of Yb(III) by fabrication of coated graphite electrode based on newly synthesized hexaaza macrocyclic ligand [J]. Analytica Chimica Acta, 2009, 643(1-2): 74-82.
- [7] GALE T F. The embryotoxicity of ytterbium chloride in golden hamsters [J]. Teratology, 1975, 11(3): 289–295.
- [8] MATLOCK M M, HOWERTON B S, ATWOOD D A. Chemical precipitation of heavy metals from acid mine drainage [J]. Water Research, 2002, 36(19): 4757–4764.
- [9] LIANG Tao, DING Shi-ming, SONG Wen-chong, CHONG Zhong-yi, ZHANG Chao-sheng, LI Hai-tao. A review of fractionations of rare earth elements in plants [J]. Journal of Rare Earths. 2008. 26(1): 7–15.
- [10] KONDO K, KAMIO E. Separation of rare earth metals with a polymeric microcapsule membrane [J]. Desalination, 2002, 144(1-3): 249-254.
- [11] JEPPESEN T, SHU L, KEIR G, JEJATHEESAN V. Metal recovery from reverse osmosis concentrate [J]. Journal of Cleaner Production, 2009, 17(7): 703-707.
- [12] MINOWA H, EBIHARA M. Separation of rare earth elements from scandium by extraction chromatography: Application to radiochemical neutron activation analysis for trace rare earth elements in geological samples [J]. Analytica Chimica Acta, 2003, 498(1–2): 25–37.
- [13] YANG Hua. Summarization of rare earth coordination complexes and their application [J]. Chinese Rare Earths, 2010, 31(3): 87–92. (in Chinese)
- [14] XIONG Chun-hua, YAO Cai-ping. Preparation and application of acrylic acid grafted polytetrafluoroethylene fiber as a weak acid cation exchanger for adsorption of Er(III) [J]. Journal of Hazardous Materials, 2009, 170(2–3): 1125–1132.
- [15] LIN S H, JUANG R S. Adsorption of phenol and its derivatives from

- water using synthetic resins and low-cost natural adsorbents: A review [J]. Journal of Environmental Management, 2009, 90(3): 1336–1349.
- [16] VLASENKO NV, KOCHKIN Y N, TOPKA A V, STRIZHAK P E. Liquid-phase synthesis of ethyl tert-butyl ether over acid cation-exchange inorganic-organic resins [J]. Applied Catalysis A: General, 2009, 362(1-2): 82-87.
- [17] CHIARLE S, RATOO M, ROVATTI M. Mercury removal from water by ion exchange resins adsorption [J]. Water Research, 2000, 34(11): 2971–2978.
- [18] PLAZINSKI W. Applicability of the film-diffusion model for description of the adsorption kinetics at the solid/solution interfaces [J]. Applied Surface Science, 2010, 256(17): 5157–5163.
- [19] OFOMAJA A E, NAIDOO E B, MODOSE S J. Dynamic studies and pseudo-second order modeling of copper(II) biosorption onto pine cone powder [J]. Desalination, 2010, 251(1–3): 112–122.
- [20] DIZGE N, KESKINLER B, BARLAS H. Sorption of Ni(II) ions from aqueous solution by Lewatit cation-exchange resin [J]. Journal of Hazardous Materials, 2009, 167(1–3): 915–926.
- [21] PIMENTEL P M, GONZALEZ G, MELO M F A, MELO D M A, SILVA C N J, ASSUNCAO A L C. Removal of lead ions from aqueous solution by retorted shale [J]. Separation and Purification Technology, 2007, 56(3): 348–353.

- [22] AGRAWAL A, SAHU K K, PANDEY B D. Systematic studies on adsorption of lead on sea nodule residues [J]. Journal of Colloid and Interface Science, 2005, 281(2): 291–298.
- [23] KULA I, UGURLU M, KAEAOGLU H, CELIK A. Adsorption of Cd(II) ions from aqueous solutions using activated carbon prepared from olive stone by ZnCl<sub>2</sub> activation [J]. Bioresource Technology, 2008, 99(3): 492–501.
- [24] HU Xiao-jun, LI Yu-shuang, WANG Yan, LI Xin-xin, LI Hui-ying, LIU Xiao, ZHANG Pin. Adsorption kinetics, thermodynamics and isotherm of thiacalix[4]arene-loaded resin to heavy metal ions [J]. Desalination, 2010, 259(1-3): 76-83.
- [25] XIAO Kang, WANG Xiao-mao, HUANG Xia, WAITE T D, WEN Xiang-hua. Analysis of polysaccharide, protein and humic acid retention by microfiltration membranes using Thomas' dynamic adsorption model [J]. Journal of Membrane Science, 2009, 342(1-2): 22-34
- [26] ZHOU Shao-li, HE Yan, YANG Ya-ting. Study on the adsorption behavior and mechanism of Cu(II) on fulvic acid [J]. Applied Chemical Industry, 2010, 39(2): 244–250. (in Chinese)
- [27] NASIR M H, NADEEM R, AKHTAR K, HANIF M A, KHALID A M. Efficacy of modified distillation sludge of rose (Rosa centifolia) petals for lead(II) and zinc(II) removal from aqueous solutions [J]. Journal of Hazardous Materials, 2007, 147(3): 1006–1014.

# SQD-85 树脂对水溶液中镱(III)的吸附

熊春华, 王国涛, 姚彩萍

浙江工商大学 应用化学系, 杭州 310012

摘 要:用化学和红外光谱等方法研究 SQD-85 树脂对镱(III)的吸附和解吸行为,探讨溶液 pH、镱(III)初始浓度、温度以及吸附时间对吸附量的影响。结果表明,SQD-85 树脂在 pH 5.5 的 HAc-NaAc 缓冲体系中对镱(III)的吸附效果最佳,测得树脂在 308 K 时的静态饱和吸附量为 347.6 mg/g;等温吸附符合 Langmuir 模型;吸附动力学符合假二级动力学模型。热力学参数表明,SQD-85 树脂吸附镱(III)是自发的吸热过程。动态实验结果符合 Thomas模型。当用 1.0 mol/L HCl 作解吸剂时,解吸率可达 97.3%。因此,使用 SQD-85 树脂可以有效地去除和回收水溶液中的镱(III)。

关键词: SQD-85 树脂; 吸附; 镱(III); 动力学; 热力学; 机理

(Edited by LI Xiang-qun)